Effects of TiO_2 Addition on the Electrochemical Performance of the Overlay Welded High-manganese Steel Cladding

Jianglong Yi[1,a], Kai Wang[2], Ben Niu[1], Xinxin Wang[1],Jianyi Wang[1] and Chunlin Dong[1]

[1] *Guangdong Welding Institute (China-Ukraine E. O. Paton Institute of Welding) Guangdong Provincial Key Laboratory of Advanced Welding Technology,*
[2] *Foshan University*

Abstract. Series of overlay flux-cored wires with different content of TiO_2 were fabricated, and different claddings of high-manganese steel are welded by flux cored arc welding (FCAW). The influences of TiO_2 addition on the electrochemical behaviour of the FCAW claddings over a high-manganese steel were studied. The results demonstrate that all the LPR values of the overlay welded claddings are higher than that of the base metal. However, the LPR values did not increase with the addition of TiO_2. The EIS simulation results indicate that the addition of titanium dioxide improves the corrosion resistance of the high-manganese steel cladding, and the trends of the Rp values is highly consistent with the change of LRP value. At the same time, the grain refinement was achieved by the TiO_2 addition. In conclusion, the proper content of the titanium dioxide in high-manganese steel cladding contributes to its high LRP and Rp values, in this paper, the suitable content of the TiO_2 addition is 20g (0.2wt. %).

1 Introduction

It is a well-known fact that overlay welding is an excellent technique to improve the surface properties of a substrate. There are many remanufacturing technologies used to accomplish the overlay weld, such as flux cored arc welding, plasma arc welding, electroslag welding and Laser welding [1,2]. For example, a cladding weld of high-manganese steel overlaid on the surface of a carbon steel can strengthen the hardness, wear resistance and crack resistance, which is widely used in many fields such as machinery, metallurgy and mining equipment. However, because of the harsh working condition, those high-manganese steel claddings were easy to damage caused by corrosion, fatigue, and stress corrosion cracking.

In order to improve the corrosion resistance, many elements have been added into the base metal of high-manganese austenitic steels. Such as Al, Cr, Cu, and Mo, which improve the tendency to form passive films on the steel surface [3-5]. However, there are few researches focused on the effects of TiO_2 addition, especially for the electrochemical performance of the overlay welded high-manganese steel cladding. Many researchers have reported that the addition of titanium dioxide can affect the characteristics of the high-manganese steel cladding. This paper aimed to investigate the influence of TiO_2 addition on electrochemical behavior of the high-manganese steel.

In this study, we fabricate series of overlay flux-cored wire with different content of TiO_2, and made different claddings of high-manganese steel using FCAW. The linear polarization for different

[a] Corresponding author: yijl@gwi.gd.cn

deposited metals on the Q235A steel were tested, aim to investigate the effect of the TiO_2 addition on the corrosion properties of the overlay weled high-manganese steel claddings.

2 Experimental

Titanium dioxide powder of -200μm mesh (99.7% purity level) was added to the base flux-cored wire in the range from 10g (0.1wt. %) to 40g (0.4wt. %) %, the major chemical composition of the weld metal of base overlay flux-cored wire was listed in Table 1. The Q235A steel according to Chinese standard GB/T11253-2007 was used as the experimental base metal with the size of 200 mm × 100 mm × 10 mm , and the chemical composition was listed in Table 2. The different claddings were obtained by FCAW with the following welding parameters as shown in table 3. Using the EWM (Phoenix 521 forceArc puls DW) as the welding machine and use the mixture of 80% Ar+20%CO_2 as protecting gas. The plate was cladded up to a thickness of 15 mm. The prepared claddings were cut to different pieces for microstructure observation and electrochemical measurement by linear cutting. The specimens for metallographic examination were mechanically polished using standard metallographic procedure and etched with a 4 vol% nital solution.

After cladding the welded samples were cut to prepare the electrochemical test with the size of 10 mm × 10 mm × 0.5 mm. The LP and EIS testes were carried out by an Autolab PGSTAT302N electrochemical workstation. And a three-electrode system was used to test the EIS corrosion properties. Using the cladded sample as the working electrode, the Pt plate as the auxiliary electrode, the reference electrode was Ag/AgCl (3 mol/L KCl), and use the 3.5 wt.% NaCl water solution as the test electrolyte. The working electrode was soaked in the electrolyte for 30min before electrochemical test, and set the open circuit potential (OCP) as the EIS mode over a frequency range of 10^4~10^{-2} Hz. While the EIS test was finished, all samples were immediately charactered by SEM analysis (JEOL, JXA-8100).

3 Results and discussion

3.1 Microstructure characterization

The micrograph of cladding metals made by the addition of TiO_2 and without addition of TiO_2 are presented in Fig.1. The microstructures of the entire clad layer revealed austenite structure. It is observed that the claddings fabricated by the addition of 20g TiO_2 (0.2 wt. %) and 30g TiO_2 (0.3 wt. %) resulted in fine equiaxed grains compared to the others. When increasing the TiO_2 addition to 40g (0.4 wt. %), the fine equiaxed grains disappear, and the grain size also become larger, which might be contributed by the generate of fine particles such as TiC, TiN [6].

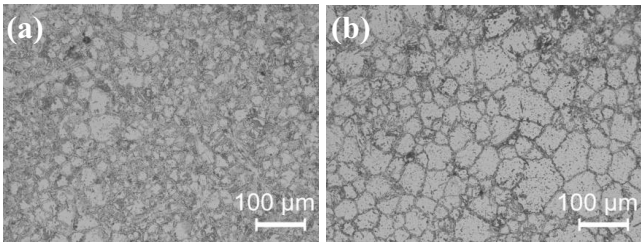

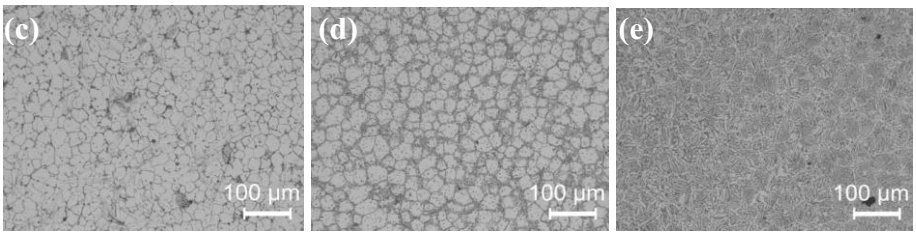

Figure 1. Optical microstructure of the five clad layer a) 0g TiO_2 (0 wt. %) addition; b) 10g TiO_2 (0.1 wt. %) addition; c) 20g TiO_2 (0.2 wt. %) addition; d)30g TiO_2 (0.3 wt. %) addition; e) 40g TiO_2 (0.4 wt. %) addition;

3.2 Electrochemical analysis

The linear polarization results of the different TiO_2 addition claddings are shown in Fig. 2. The LP lines of the clad layer the addition of 30g TiO_2 (0.3 wt. %) is the most stable with the most positive self-corrosion potential, compared with those of the overlay welded metals. The linear polarization resistances (LPR) values are shown in Tab.4, and the results demonstrate that all the LPR values of the overlay welded claddings are higher than that of the base metal. However, the LPR values are not increased with the addition of TiO_2.The LPR value of the clad layer of 1# at 10g TiO_2 addition is 11356.35 Ohm.cm^2, while the 2# presents a similar LRP value of 10467.56 Ohm.cm^2 to the LPR value of 1#. Both of them are extremely higher than the others. As the TiO_2 increased to 40g (0.4 wt. %) and 50g (0.5 wt. %), the LRP value decreased sharply to 6273.13 and 5024.23 Ohm.cm^2, respectively.

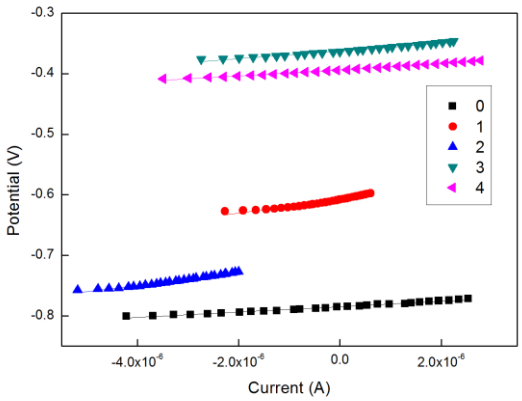

Figure 2. Linear polarization curves of the different clad layer

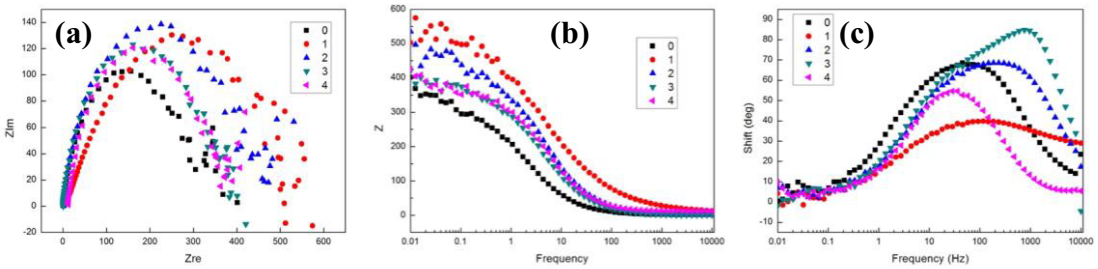

Figure 3. (a) Nyquist, (b) Bode and (c) Bode-phase plots of the five clad layer at open-circuit potential. a) 0g TiO_2 (0 wt. %) addition; b) 10g TiO_2 (0.1 wt. %) addition; c) 20g TiO_2 (0.2 wt. %) addition; d)30g TiO_2 (0.3 wt. %) addition; e) 40g TiO_2 (0.4 wt. %) addition;

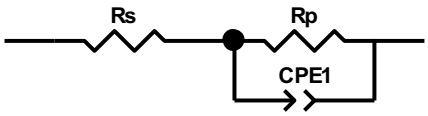

Figure 4. Best equivalent circuit used to model the experimental EIS data

Table 1. Chemical composition of the weld metal of base overlay flux-cored wire %

C	Si	Mn	Cr	Ni	V	Mo	Al
0.032	0.063	12.39	11.28	1.23	0.38	0.79	0.085

Table 2. Chemical composition of Q235 steel %

C	Si	Mn	P	S
0.14~0.22	≤0.30	0.30~0.65	≤0.045	≤0.050

Table 3. Welding parameters of the welding process

Parameter	Value
Current (A)	240-260
Voltage (V)	24-26
Electrode polarity	DCEP
Filler wire diameter (mm)	1.6
Interpass temperature (°C)	150
Welding speed (mm·s-1)	6.8

Table 4. The linear polarization resistances of the weled metal at different TiO2 Adddition

No.	TiO_2 Adddition	LPR (Ohm.cm2)
0#	0g	4418.89
1#	10g	11356.35
2#	20g	10467.56
3#	30g	6273.13
4#	40g	5024.23

Table 5. Variations in the impedance parameters of the EIS tested samples

	0#	1#	2#	3#	4#
	Value	Value	Value	Value	Value
Rs ($\Omega \cdot cm^2$)	1.27	1.12	7.17	0.33	11.78
Rp($\Omega \cdot cm^2$)	323.9	437.4	554.6	343.2	359.9
CPE1T(mf)	5.57×10-4	2.09×10-4	3.66×10-4	1.66×10-4	2.49×10-4
CPE1-P	0.82	0.81	0.54	0.91	0.81

The EIS measurements were conducted for cladded samples in a 3.5% NaCl solution in order to evaluate the corrosion protection performance of the overlay welded high-manganese steel. Figures 3 show the results for Nyquist, Bode, and Bode-phase plots. It was possible fit well with all the impedance spectra using the equivalent circuit model shown in Fig. 4.

The Nyquist plots of all the clad layer show similar semicircles, represented as the capacitive arc. The diameter of the semicircle of the overlay welded claddings with TiO_2 addition was bigger than that of the base metal without TiO_2 addition. The 1# and 2# sample show similar and also the biggest semicircle diameter which reflected the best passivation behavior. Moreover, the imperfect semicircle diameter for the clad layer of 1# and 2# is higher than that of the 3# and 4#, which agrees well with the LPR values.

As seen in Fig. 3b, the Bode plots show higher electrical resistance value at the low-frequency range, which represent the stronger corrosion resistance and consistent with the result of the above

Nyquist plots. One time-constant was observed on the bode plots of all samples (only one maximum phase lag at the middle frequency range). As can be seen from the Bode-phase curves, except the 3# all the clad layer exhibit certain constant plots at the middle frequency range [7]. Also, the phase angles values remained far below to 80° except the 3#, which indicated the formation and growth of the corrosion pits at middle frequency [8, 9]. And the maximum phase angles values of 3# was over 80°, which revealed the formation of a passive film. In other words, it means a pure or ideal capacitive response [10].

Figure 4 shows equivalent circuit best describing the electrochemical processes [11]. In this equivalent model, Rs is the solution resistance; Rp stands for the resistance of the sample in the solution, and CPE1 counts for the constant phase element corresponding to the capacitance of the corrosion pits. As the most important characteristic of all the EIS value, the polarization resistance Rp represent the resistant ability to against the corrosion [12, 13]. Table 5 shows all the values of equivalent circuit elements of the cladding samples in 3.5% NaCl solution. The highest value of Rp was reached to 554.6 Ω•cm2, which indicated the 2# with 20g TiO_2 (0.2 wt. %) possesses best anti-corrosion ability of the entire clad layer. The simulation results demonstrate that the addition of titanium dioxide improves the corrosion resistance of overlay welded high-manganese steel cladding.

3.3 Corrosion morphologies analysis

Fig. 5 shows SEM images of the corrosion morphologies of the high-manganese steel cladding with different TiO_2 addition after the electrochemical tests in a 3.5% NaCl solution. It is apparent that, the rust films formed at all the test samples. The rust films became increasingly dense and uniform as the increase of the TiO_2 addition. Fig. 4a shows the morphology of the rust presented in a loose porous structure, and obvious cracking phenomena can be easily seen on the clad layer surface. It is obvious that a dense passive film without crack can be observed on the surface of the cladded sample with 20g TiO_2 (0.2 wt. %) addition, which prevents the corrosive penetration trend of the experimental solutions. Meanwhile, this phenomenon well explained and consistent with the close LRP value and EIS measurements result. It is found that there are more corrosive crack appears on the surfaces, as increase the addition amount of the TiO_2. It will accelerate the corrosive solution penetration trend of the experimental solutions [14].

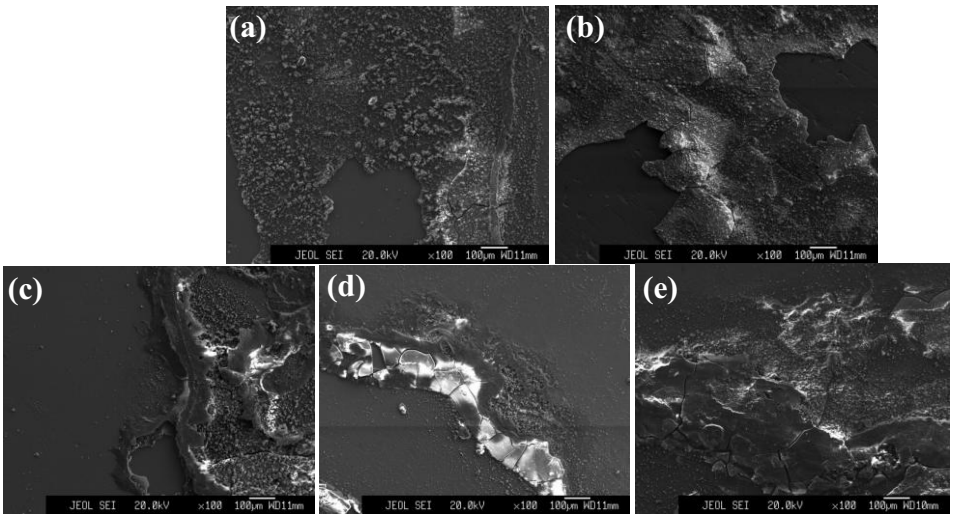

Figure 5. The corrosion morphology of the five claddings after the electrochemical tests ×500a) 0g TiO_2 (0 wt. %) addition; b) 10g TiO_2 (0.1 wt. %) addition; c) 20g TiO_2 (0.2 wt. %) addition; d)30g TiO_2 (0.3 wt. %) addition; e) 40g TiO_2 (0.4 wt. %) addition;

4 Conclusion

The results demonstrate that all the LPR values of the overlay welded claddings are higher than that of the base metal. However, the LPR values do not increase with the addition of TiO_2. To simulate the measured impedance EIS data, the equivalent circuit was used, the simulation results indicate that the addition of TiO_2 improves the corrosion resistance of the high-manganese steel cladding and the trends of the Rp values is highly consistent with the change of LRP value. At the same time, the grain refinement is achieved by the TiO_2 addition. In conclusion, the proper content of the TiO_2 in high-manganese steel cladding contributes to its high resistance values and good corrosive surface morphology, as in this paper, the suitable content of the TiO_2 addition is 20g (0.2wt. %). As resulted in the increase of the polarization resistance to present a similar electrochemical behavior as the high-manganese steel cladding.

Acknowledgements

This research was supported by the technical project of Guangdong (2014B050503004, 2013B050800028, 2015B050502005, 2016B090918120, 2012A061400011), the Guangzhou Science and Technology research project (201510010101, 201508030024, 2015B050502003), The Scientific Program of GDAS (2016GDASPT-0205) and the National Natural Science Foundation of China (No. 51601043).

References

1. N.V. Rao, G.M. Reddy, S. Nagarjuna, Mater. Des. **32**,4 (2011).
2. Metals hand book. *Welding, brazing and soldering*, 9th ed. vol. 6. Metals Park (OH, USA): ASM; (1983)
3. M.B. Kannan, R.K.S. Raman, and S. Khoddam, Corros. Sci., **50**,10 (2008)
4. Y.S. Zhang, X.M. Zhua, and S.H. Zhong, Corros. Sci., **46**, 4 (2004)
5. T. Dieudonne, L. Marchetti, M. Wery, F. Miserque, M. Tabarant, J. Chene, C. Allely, P. Cugy, and C.P. Scott, Corros. Sci. **83**,7 (2014)
6. G. Mallaiah, P. R. Reddy, A. Kumar, Procedia Mater. Sci. **6**, (2014)
7. J. Soltis, K.A. Lichti,. Corros. Sci. **68**, (2013)
8. L.R. Bhagavathi, G.P. Chaudhari, S.K. Nath, Mater. Des., **32**,1 (2011)
9. A. Fattah-alhosseini, S. Vafaeian, J. Alloys Compd., **639** ,(2015)
10. H. Y. Ha, M. H. Janga, T. H. Lee, J. Moon, Corros. Sci. **89**, (2014)
11. F. Pastorek, K. Borko, S. Fintova, D. Kajsnek, B. Hadzima, Coating, **6**,4 (2016)
12. M. Mhaede, F. Pastorek, B. Hadzima, Mater. Sci. Eng., C, **39,** (2014)
13. E. A. Avila, L. A. Rocha, Mater. Sci. Forum, **492**, (2005)
14. G. Q. Su, X. H. Gao, L. X. Du, et al. Int J Electrochem Sc, **11**, 11, (2016)